

TOR and PKA Signaling Pathways Converge on the Protein Kinase Rim15 to Control Entry into G₀

Short Article

Ivo Pedruzzi,^{1,3} Frédérique Dubouloz,^{1,3}
Elisabetta Cameroni,¹ Valeria Wanke,¹
Johnny Roosen,² Joris Winderickx,²
and Claudio De Virgilio^{1,*}

¹Department of Medical Biochemistry
CMU

University of Geneva
1211 Geneva 4
Switzerland

²Functional Biology
Katholieke Universiteit Leuven
Leuven-Heverlee
B-3001 Flanders
Belgium

Summary

The highly conserved Tor kinases (TOR) and the protein kinase A (PKA) pathway regulate cell proliferation in response to growth factors and/or nutrients. In *Saccharomyces cerevisiae*, loss of either TOR or PKA causes cells to arrest growth early in G₁ and to enter G₀ by mechanisms that are poorly understood. Here we demonstrate that the protein kinase Rim15 is required for entry into G₀ following inactivation of TOR and/or PKA. Induction of Rim15-dependent G₀ traits requires two discrete processes, i.e., nuclear accumulation of Rim15, which is negatively regulated both by a Sit4-independent TOR effector branch and the protein kinase B (PKB/Akt) homolog Sch9, and release from PKA-mediated inhibition of its protein kinase activity. Thus, Rim15 integrates signals from at least three nutrient-sensory kinases (TOR, PKA, and Sch9) to properly control entry into G₀, a key developmental process in eukaryotic cells.

Introduction

The highly conserved TOR proteins control growth of proliferating yeast, flies, and mammalian cells in response to growth factors and/or nutrients (Jacinto and Hall, 2003). In yeast, TOR depletion or treatment with rapamycin results in growth arrest that is associated with physiological changes, which are characteristic of stationary phase (G₀) cells (Werner-Washburne et al., 1993). These include G₁ cell cycle arrest, repression of general transcription and mRNA translation, induction of a defined set of stress response genes (e.g., *SSA3*, *HSP26*, and *HSP12*), and synthesis of glycogen and trehalose (Werner-Washburne et al., 1993; Jacinto and Hall, 2003). While TOR controls some readouts via the type 2A (Pph21 and Pph22) or type 2A-related (Sit4) protein phosphatases (PP2As) and their regulator Tap42 (Di Como and Arndt 1996; Jiang and Broach 1999), the effector pathway(s) that controls readouts such as re-

pression of Pol II transcription (and other G₀-associated changes) remain still elusive.

The PKA pathway constitutes another key signaling pathway that controls growth of proliferating yeast in response to nutrients. The mechanism by which PKA controls growth, however, is still an issue of conjecture, and further elucidation of this process will certainly depend on the identification of downstream effectors of PKA. One such effector, the protein kinase Rim15, is required for proper establishment of the G₀ program and is inhibited by PKA-mediated phosphorylation under conditions of nutrient abundance (Reinders et al., 1998). Interestingly, downregulation of PKA following nutrient limitation liberates Rim15 from PKA-inhibition and results in activation of G₀-related changes, which are strikingly similar to the changes observed following rapamycin treatment. These findings suggest a model in which the TOR pathway may converge on a component and/or target of the PKA pathway to control entry into G₀.

Here we show that proper entry into G₀ following TOR inactivation depends on the PKA target Rim15. TOR prevents induction of Rim15-dependent responses via a Sit4-independent mechanism, which alters the phosphorylation status of Rim15 and thereby inhibits nuclear accumulation of Rim15. Moreover, we demonstrate that nucleocytoplasmic distribution of Rim15 is regulated by the yeast protein kinase B (PKB/Akt) homolog Sch9. Thus, Rim15-controlled developmental processes are fine-tuned by integration of signals that are transmitted via at least three key nutrient-sensory kinases, i.e., TOR, PKA, and Sch9.

Results and Discussion

TOR Prevents Induction of Rim15-Dependent G₀ Traits

To investigate whether TOR may feed into the PKA pathway upstream, or at the level of Rim15, we first studied a role of Rim15 in TOR-dependent phenotypes. Wild-type and *rim15Δ* cells were grown in rich medium to early logarithmic phase, treated with rapamycin (0.2 μg ml⁻¹) to inactivate TOR proteins, and assayed for G₁ cell cycle arrest, induction of *SSA3*, *HSP26*, and *HSP12*, and synthesis of glycogen and trehalose. While wild-type cells were blocked in G₁ (Figure 1A), strongly induced *SSA3*, *HSP26*, and *HSP12* transcripts (Figure 1B), and produced high levels of glycogen (Figure 1C) following treatment with rapamycin, *rim15Δ* cells were (despite an early response to rapamycin) defective for proper G₁ arrest (particularly 4 and 6 hr following rapamycin treatment; Figure 1A) and showed no significant increase in the levels of *SSA3*, *HSP26*, and *HSP12* transcripts and of glycogen even after 6–8 hr treatment with rapamycin (Figures 1A–1C). Similarly, a 6 hr rapamycin treatment caused trehalose levels to increase in wild-type cells, but not in the corresponding *rim15Δ* mutant (Figure 1D). Loss of Rim15, however, did not impair the ability of the cells to downregulate translation initiation following TOR inactivation (assayed by polysome profile analysis), nor allow cells to grow on (0.2 μg ml⁻¹) rapamycin.

*Correspondence: claudio.devirgilio@medecine.unige.ch

³These authors contributed equally to this work.

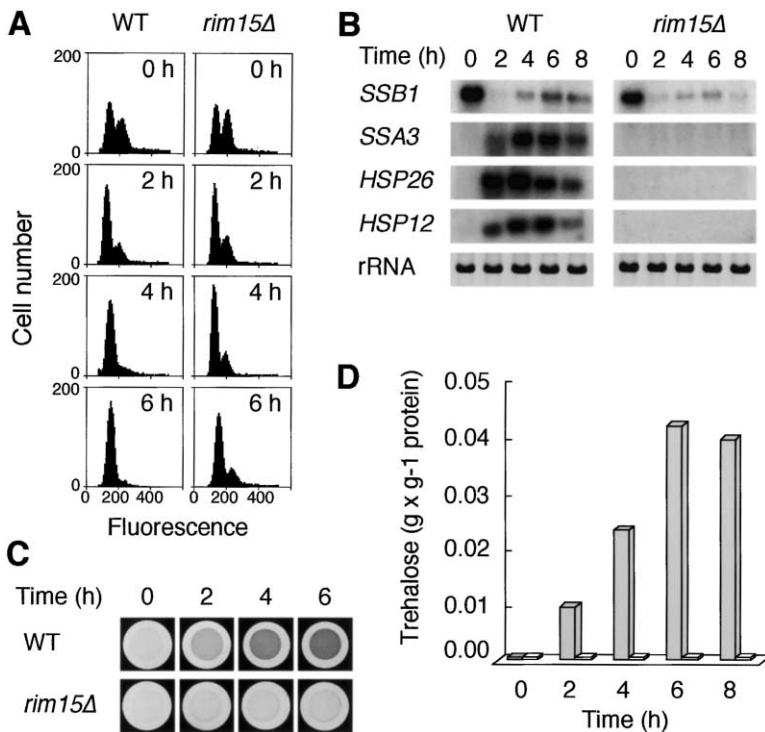


Figure 1. Rim15 Is Required for Entry into G₀ following TOR Inactivation by Rapamycin

(A) DNA content determined by flow cytometry; (B) Northern analysis of indicated genes; (C) glycogen levels (visualized after exposure for 1 min to iodine vapor); and (D) trehalose levels of exponentially growing (OD₆₀₀ < 0.5) wild-type (JK9-3da; gray bars) and isogenic *rim15Δ* (IP11; open bars) mutant cells following treatment with rapamycin (0.2 μg ml⁻¹) for the times indicated.

mycin-containing plates (data not shown). Thus, while TOR appears to regulate growth via Rim15-independent mechanisms, it prevents induction of Rim15-dependent G₀ traits.

TOR Controls Rim15 Function via a PKA- and Sit4-Independent Mechanism

Since Rim15 kinase activity is under direct, negative control of PKA (Reinders et al., 1998), we tested whether the rapamycin-induced, Rim15-dependent transcriptional response can be modulated by mutations that affect PKA activity. Interestingly, we found that loss of Ras2, an activator of adenylate cyclase in yeast, caused partial derepression of *HSP12* and *SSA3* and slightly enhanced the rapamycin-induced activation of *SSA3*, *HSP26*, and *HSP12* (Figure 2A). In contrast, constitutive activation of PKA due to loss of the regulatory PKA subunit Bcy1 or following introduction of the dominant active *RAS2^{Val19}* allele (data not shown) almost completely abolished rapamycin-induced induction of all three genes (Figure 2A). The TOR signaling pathway may therefore control expression of these genes by regulating a component of the PKA pathway. In order to examine whether this presumed component functions at the level or upstream of PKA and/or Rim15, we investigated whether the rapamycin-induced transcriptional activation of *SSA3*, *HSP26*, and *HSP12* depends on the presence of PKA and/or Rim15 by using *pka*⁻ strains rendered viable through deletion of either *YAK1* or *RIM15* (Reinders et al., 1998; Garrett and Broach, 1989). In the absence of PKA, rapamycin-inducibility of all three genes under study remained high (in the *pka*⁻ *yak1Δ* strain) and was still strongly dependent on the presence of Rim15 (in the *pka*⁻ *rim15Δ* strain; Figure 2B). Thus,

part of the role of TOR in preventing G₀ entry is mediated by PKA-independent inhibition of Rim15 function.

To determine whether TOR-mediated control of Rim15 requires any of the known PP2A TOR effectors, we investigated whether loss of Sit4 or Pph21 and Pph22 affected basal and/or rapamycin-induced levels of *SSA3*, *HSP26*, and *HSP12* transcription. We found that loss of Sit4 did not significantly alter the cells' basal or rapamycin-induced *SSA3*, *HSP26*, and *HSP12* transcript levels (Figure 2C), indicating that TOR regulates Rim15 function via a Sit4-independent pathway. In agreement with this notion, we also found rapamycin-sensitive, Sit4-dependent genes—including Gln3 (e.g., *DAL5* and *PUT1*) as well as Rtg3 target genes (e.g., *PYC1* and *CIT2*; Düvel et al., 2003)—to be regulated largely independently of Rim15 (Figure 2D). Interestingly, loss of both Pph21 and Pph22 strongly enhanced the basal levels of *SSA3*, *HSP26*, and *HSP12* transcripts in exponentially growing cells, indicating that Pph21 and Pph22 are implicated in inhibition of basal transcription of Rim15-controlled genes (Figure 2E). Irrespective of these high basal transcription levels, however, all three genes remained rapamycin-inducible in the *pph21Δ pph22Δ* double mutant (Figure 2E). Thus, even though the mechanism by which Pph21 and Pph22 control basal transcription levels of *SSA3*, *HSP26*, and *HSP12* remains unknown at present, our results show that rapamycin-induced transcriptional induction of Rim15-controlled genes does not require the known PP2A TOR effectors Pph21 and Pph22 or Sit4. In line with this conclusion, we also found that a semidominant, rapamycin-resistant mutation in the PP2A regulatory Tap42 protein (i.e., *tap42-11*; Di Como and Arndt, 1996) did not prevent induction of *SSA3*, *HSP26*, and *HSP12* transcription following rapamycin treatment (Figure 2C).

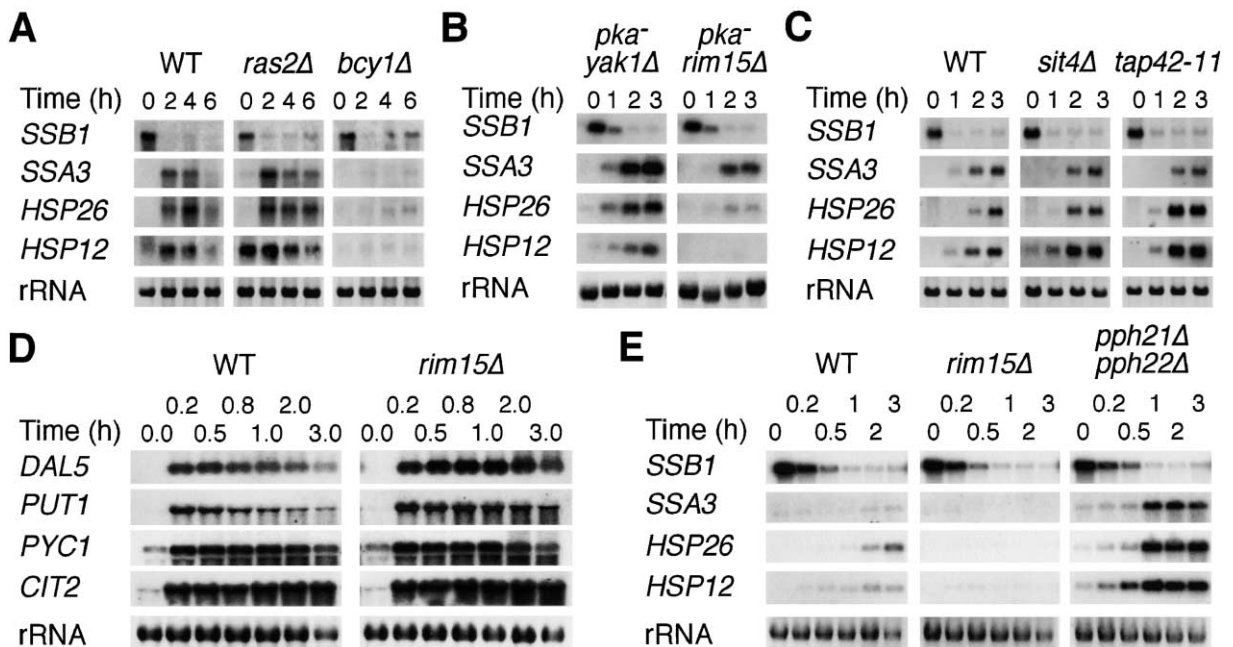


Figure 2. Transcriptional Activation of Rim15-Controlled Genes following TOR Inactivation Does Not Depend on Known PP2A TOR Effectors and Is Negatively Regulated by PKA

SSB1, *SSA3*, *HSP26*, and *HSP12*, or *DAL5*, *PUT1*, *PYC1*, and *CIT2* transcript levels were determined in cells growing exponentially at 30°C (*tap42-11* mutant at 24°C) on rich medium and treated with rapamycin (0.2 μg ml⁻¹) for the times indicated. The decrease in *SSB1* transcript level was used as internal control for rapamycin function. Strains used in (A) were wild-type (SP1), *ras2Δ* (IP16), and *bcy1Δ* (T16-11A); in (B) *pka- yak1Δ* (CDV80-2D) and *pka- rim15Δ* (CDV80-15A); in (C) wild-type (JK9-3da), *sit4Δ* (TS64-1a), and *tap42-11* (TS54-5a); in (D) wild-type (W303-1A) and *rim15Δ* (CDV115); and in (E) wild-type (W303-1A), *rim15Δ* (CDV115), and *pph21Δ pph22Δ* (YP0607WH). In order to visualize the strong differences between expression of genes in wild-type and *pph21Δ pph22Δ* cells, Northern blots in (E) were all equally exposed, but for a shorter time than in all other experiments. Strains used in individual panels are isogenic.

TOR but Not PKA Regulates Nucleocytoplasmic Distribution of Rim15

To investigate the mechanism by which TOR inactivates Rim15, we transformed various strains with a *GFP-RIM15* plasmid and visualized localization of the corresponding GFP-Rim15 fusion protein in cells treated with rapamycin for various time periods. In untreated cells, GFP-Rim15 was detected predominantly in the cytoplasm and appeared excluded from the nucleus. Within 30 min following rapamycin treatment, however, localization of GFP-Rim15 was predominantly nuclear (Figure 3A), which is consistent with the effects of rapamycin on transcription of Rim15-dependent genes (i.e., measurable induction at 30–45 min following rapamycin treatment; Figure 2E). Moreover, rapamycin-induced nuclear accumulation of GFP-Rim15 was defective in a rapamycin-resistant *TOR1-1* mutant (Helliwell et al., 1994), indicating that the observed effect is due to TOR inactivation. Notably, TOR has been suggested to control subcellular localization of proteins by two different processes, namely prevention of nuclear import (e.g., of Gln3 and Rtg3; Komeili et al., 2000; Crespo et al., 2002) and stimulation of nuclear export (e.g., of Msn2; Görner et al., 2002; Düvel et al., 2003). In the latter case, nuclear appearance of a given protein following TOR inhibition depends largely on its nuclear import rate. The slight delay in rapamycin-induced nuclear appearance of Rim15 (i.e., about 20 min when compared to Gln3 or Rtg3), and possibly also Msn2 (Düvel et al., 2003), could therefore be explained by a model in which inhibition of

TOR—rather than activating nuclear import—prevents nuclear export, thus rendering nuclear appearance of Rim15 mainly dependent on a potentially slow import rate.

In order to confirm that TOR controls Rim15 function independently of PKA, we studied rapamycin-induced nuclear translocation of GFP-Rim15 in mutants that are either hyper- or hypoactive for PKA. Accordingly, we found that hyperactivation of PKA (due to expression of *RAS2^{Val19}*) had no significant effect on the rapamycin-induced nuclear translocation of GFP-Rim15 (Figure 3A). For examination of the effects of hypoactive PKA, we used a strain that was rendered responsive to extracellular cAMP by deletion of the genes encoding adenylate cyclase (*CDC35*) and low-affinity phosphodiesterase (*PDE2*). In such a strain, depletion of cAMP (and hence inactivation of PKA) for 30 min (and up to 2 hr) in the presence of rich medium did not cause a change in cytoplasmic localization of GFP-Rim15 (Figure 3B). As a control, we found nuclear import of Msn2-myc9, which is negatively regulated by PKA (Görner et al., 2002), to occur rapidly under the same conditions (Figure 3B). Thus, TOR inactivates Rim15 by preventing its access to or promoting its export from the nucleus via a process that is independent of regulated PKA activity.

TOR-Inhibition Results in Rapid Alteration of the Rim15 Phosphorylation State

How does TOR control nuclear localization of Rim15? GST-Rim15 in total cell extracts from untreated cells

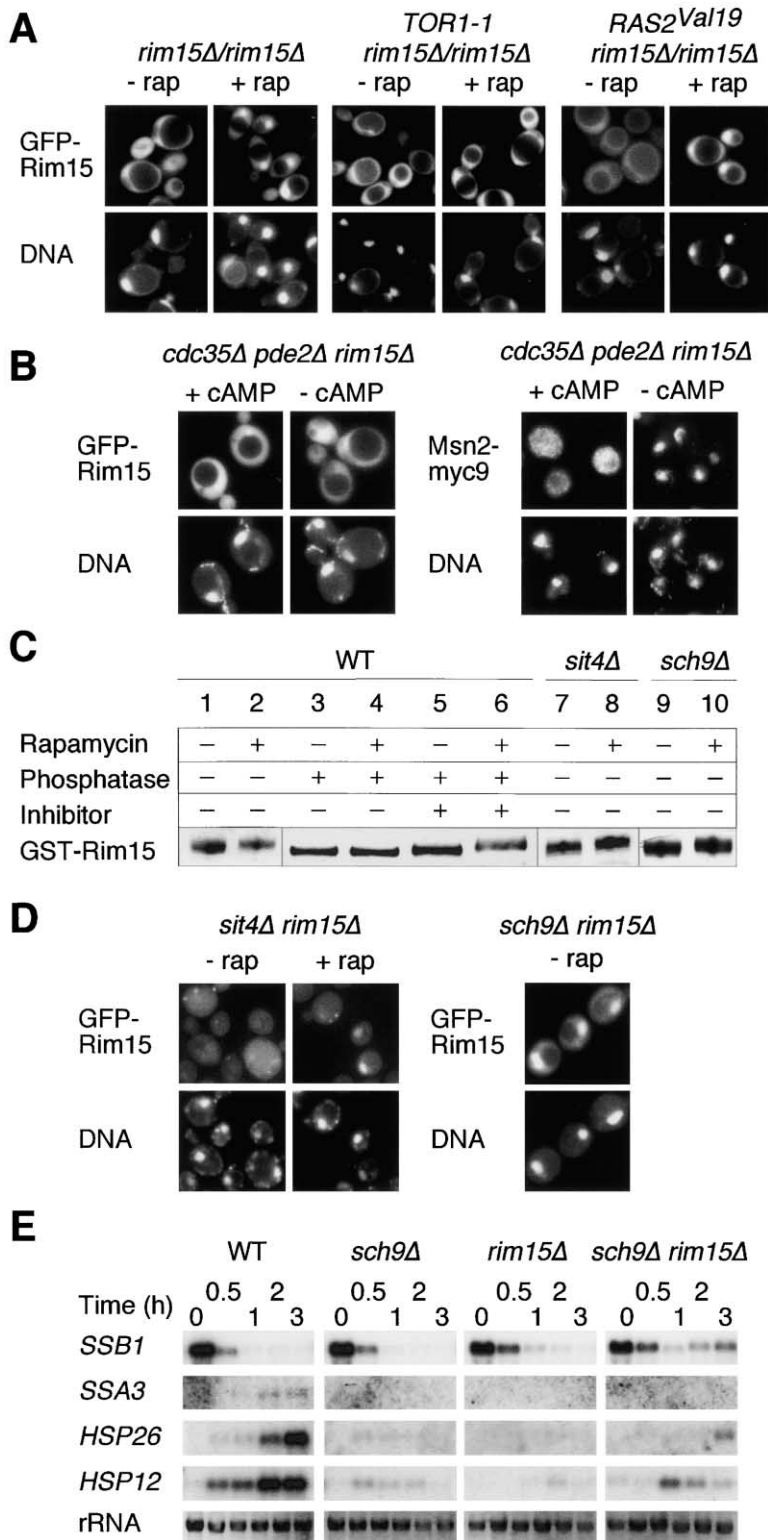


Figure 3. TOR and Sch9 but Not PKA Control Nuclear Localization of Rim15

(A) Localization of GFP-Rim15 in *rim15Δ/rim15Δ* cells (IP37) carrying a control plasmid (YEp213), a plasmid expressing the rapamycin-resistant *TOR1-1* allele, or a plasmid expressing the dominant active *RAS2^{Val19}* allele. Cells were grown on SD-medium, treated for 30 min with rapamycin (+rap) or the drug vehicle alone (-rap), and visualized by fluorescence microscopy. DNA was stained with DAPI.

(B) Localization of GFP-Rim15 and Msn2-myc9 in a *cdc35Δ pde2Δ rim15Δ* triple mutant (CDV177-3C). Cells were grown in SD-medium containing 5 mM cAMP (+) and then shifted for 30 min to the same medium without cAMP (-). Msn2-myc9 was detected by indirect immunofluorescence.

(C) Rim15 is hyperphosphorylated upon rapamycin treatment. GST-Rim15 from *rim15Δ/rim15Δ* (IP37), *sit4Δ* (YPA5H), and *sch9Δ* (TVH301) cells that were untreated (-) or treated (+) for 20 min with rapamycin was detected by immunoblotting. Whole-cell extracts were incubated with alkaline phosphatase (\pm phosphatase inhibitors).

(D) Localization of GFP-Rim15 in *sit4Δ rim15Δ* (FD6) and *sch9Δ rim15Δ* (RJ201) cells. For details see (A).

(E) *SSB1*, *SSA3*, *HSP26*, and *HSP12* transcript levels were determined in cells growing on rich medium and treated with rapamycin for the times indicated. Strains used were wild-type (W303-1A), *sch9Δ* (TVH301), *rim15Δ* (CDV115), and *sch9Δ rim15Δ* (RJ201). In all experiments, cells were grown exponentially prior to rapamycin treatment ($2 \mu\text{g ml}^{-1}$ for GFP-Rim15 localization studies and $0.2 \mu\text{g ml}^{-1}$ for all other experiments).

exhibited a higher electrophoretic mobility compared with GST-Rim15 from rapamycin-treated cells (Figure 3C, lanes 1 and 2). Phosphatase treatment of GST-Rim15 prepared from untreated and rapamycin-treated cells converted GST-Rim15 to a similar form (Figure 3C, lanes 3 and 4) that migrated faster than the correspond-

ing controls prepared in the presence of phosphatase inhibitors (Figure 3C, lanes 5 and 6). These results show that exponential-phase Rim15 is phosphorylated in the absence of rapamycin, which is in agreement with our previous findings (Reinders et al., 1998). Moreover, rapamycin treatment induces an additional change in the

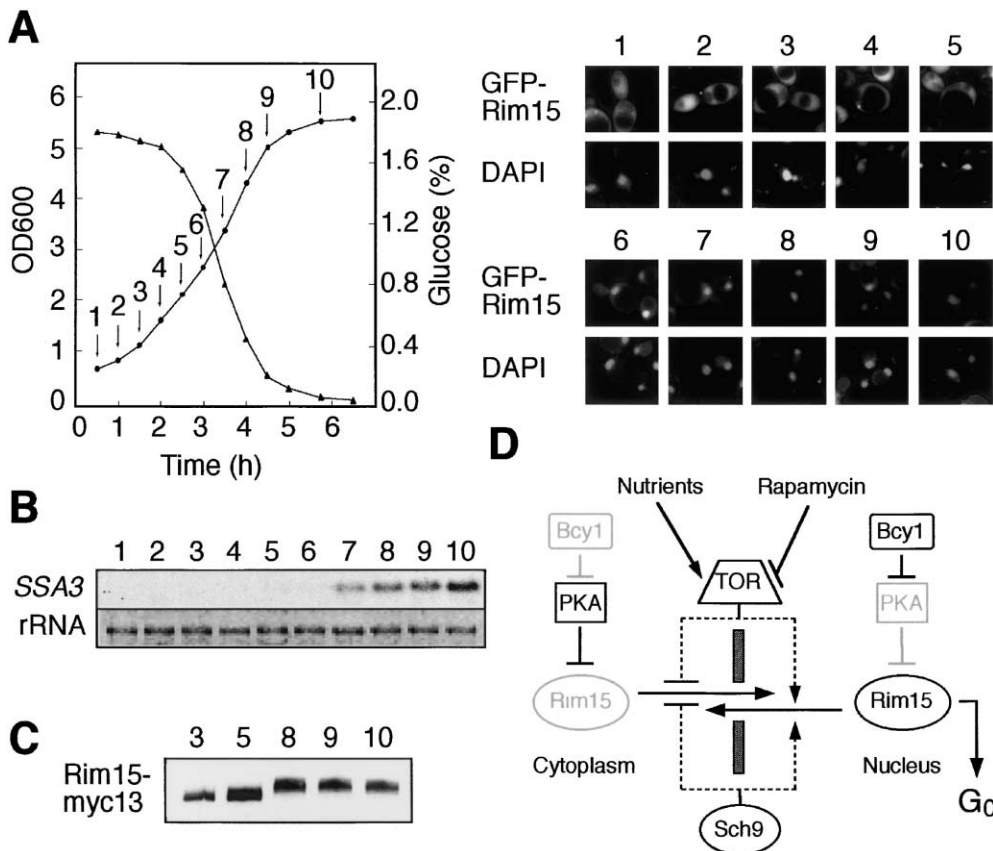


Figure 4. Glucose Limitation Triggers Hyperphosphorylation and Nuclear Accumulation of Rim15, followed by Induction of Rim15-Dependent SSA3 Transcription

(A) Diploid *rim15Δrim15Δ* (IP37) cells carrying a *GFP-RIM15* construct were grown in a batch culture on SD-medium and, at the times indicated by the numbered arrows, samples were withdrawn for glucose assays and OD₆₀₀ determinations (left panel), as well as for GFP-Rim15 localization studies (right panel). Numbers in the right panel refer to the times indicated by the numbered arrows in the left panel.

(B) Glucose-limitation-induced SSA3 transcript levels in wild-type (KT1960) cells. Numbers refer to the times and corresponding glucose concentrations indicated by the numbered arrows in (A), left panel.

(C) Wild-type strain VW1 expressing Rim15-myc13 was grown in a batch culture and samples were withdrawn for immunodetection of Rim15-myc13 at different time points. Numbers refer to the times and corresponding glucose concentrations indicated by the numbered arrows in (A), left panel.

(D) TOR, via a Sit4-independent mechanism, and Sch9 promote cytoplasmic retention and/or nuclear exclusion of the PKA target Rim15. Arrows and bars denote positive and negative interactions, respectively. Notably, in exponentially growing cells, the cytoplasm hosts low levels of Bcy1 and hence primarily free, active PKA, while the inactive PKA/Bcy1 holoenzyme appears predominantly in the nucleus (Griffioen et al., 2000). Consequently, PKA-mediated inhibition of Rim15 activity is presumably lower in the nucleus than in the cytoplasm. Gray symbols denote low activity levels of the corresponding proteins. TOR and Sch9, according to the simplest interpretation of our results, control Rim15 localization via two different mechanisms. Sch9 may impinge directly or indirectly on Rim15 localization.

phosphorylation state of Rim15, which—based on the lower electrophoretic mobility of Rim15—is likely due to phosphorylation. Interestingly, while rapamycin-induced dephosphorylation of a number of proteins occurs via the Sit4/Tap42 TOR effector branch (e.g., Npr1, Gln3, Rtg3, and Gcn2; Schmidt et al., 1998; Beck and Hall, 1999; Cherkasova and Hinnebusch, 2003; Düvel et al., 2003; Liu et al., 2003), we found rapamycin-induced phosphorylation and nuclear accumulation of Rim15 to be unaffected by the loss of Sit4 (Figure 3C, lanes 7 and 8; Figure 3D). Notably, phosphorylation following rapamycin treatment is not without precedent (e.g., Put3; Saxena et al., 2003), suggesting that TOR may regulate additional proteins via a common, new effector pathway. Taken together, we found that inhibition of the TOR kinases by rapamycin results in both rapid nuclear

accumulation of Rim15 and induction of Rim15-dependent transcription. In addition, rapamycin treatment correlates with changes in the phosphorylation state of Rim15, indicating that nucleocytoplasmic transport of Rim15 is likely to be regulated by differential phosphorylation of Rim15.

Nuclear Exclusion of Rim15 Requires the Yeast PKB Homolog Sch9

Recent evidence indicates that the yeast PKB/Akt homolog Sch9 signals the combined presence of glucose and nitrogen and impinges on PKA targets in a pathway parallel to PKA (Crauwels et al., 1997; Lorenz et al., 2000; Fabrizio et al., 2001). In this context, it was reported that life-span extension following both downregulation of PKA (in an adenylate cyclase mutant) or loss of Sch9

depends on the presence of Rim15, suggesting that Rim15 may be negatively regulated by both PKA and Sch9 (Fabrizio et al., 2001). In line with such a model, we found that loss of Sch9—which had no effect on GFP-Rim15 expression levels (data not shown)—resulted in predominantly constitutive nuclear localization of Rim15 (Figure 3D). Thus, Sch9, like TOR, is required for nuclear exclusion and/or cytoplasmic retention of Rim15. Notably, however, since rapamycin-induced phosphorylation of Rim15 appeared to occur even in the absence of Sch9 (Figure 3C, lanes 9 and 10), TOR and Sch9 are likely to regulate Rim15 function via two different mechanisms. Finally, we also studied rapamycin-sensitivity of SSA3, HSP26, and HSP12 transcription in wild-type, *rim15Δ*, *sch9Δ*, and *sch9Δ rim15Δ* cells. We found that loss of Sch9 resulted in a defect in rapamycin-induced activation of all three genes, which was independent of the presence or absence of Rim15 (Figure 3E). This rather surprising result indicates that Sch9, while acting as an inhibitor of Rim15 nuclear accumulation, formally also acts (directly or indirectly) as an activator of Rim15-controlled gene expression. In line with this interpretation, Sch9 has been found to be required for downregulation of PKA (Crauwels et al., 1997), an inhibitor of Rim15 protein kinase activity (Reinders et al., 1998). Thus, our ostensibly paradoxical data can be unified in a tantalizing model in which Sch9—in response to the nutritional status—acts as a molecular buffer system by regulating the amplitude of Rim15-dependent responses via two opposing mechanisms.

Glucose Limitation Causes Hyperphosphorylation and Nuclear Accumulation of Rim15

We have previously shown that expression driven by the postdiauxic shift (PDS) element, which confers transcriptional activation (e.g., of SSA3) following glucose limitation at the diauxic transition, is almost entirely dependent on Rim15 and its presumed target Gis1 (Pedruzzi et al., 2000). Therefore, we tested whether glucose-limitation-induced activation of SSA3 may be preceded by nuclear accumulation of GFP-Rim15. Indeed, we found that cells grown in a batch culture started to accumulate GFP-Rim15 in their nuclei when 50% of the initial amount of glucose has been consumed (Figure 4A, time point 6), which is consistent with the observed pattern of transcriptional induction of SSA3 (Figure 4B). Interestingly, we obtained similar results when growing the cells on rich media with only 1% (instead of 2%) initial glucose levels (data not shown), indicating that the underlying regulatory system may (directly or indirectly) sense the kinetics of glucose limitation, rather than the absolute glucose levels. Moreover, since glucose limitation, like rapamycin treatment, caused nuclear accumulation accompanied by hyperphosphorylation of Rim15 (Figure 4C), it is possible that TOR may have a central role in this process (Figure 4D). Thus, together with the recent observation that TOR regulates subcellular localization of proteins in response to glutamine (e.g., Gln3, Rtg3, and Ime1; Crespo et al., 2002; Colomina et al., 2003), our current data lend further support to the idea that TOR may act as a multichannel processor that differentially regulates gene expression in response to specific nutrients.

Experimental Procedures

Strains, Plasmids, and Media

Yeast strains *sit4Δ* (TS64-1a), *tap42-11* (TS54-5a), and their wild-type parent (JK9-3da), and strains *sit4Δ* (YPA5H), *pph21Δ pph22Δ* (YP0607WH), and their wild-type parent (W303-1A) were previously described (Beck and Hall, 1999; Sakumoto et al., 2002). Wild-type strains KT1960 (MAT α) and KT1961 (MATa) are *ura3*, *leu2*, *his3*, and *trp1*, and congenic to KT1112 (Stuart et al., 1994). Strains AR1-1B, SP1, T16-11A, NB13-1D, SGP406, and PD6517 were also described earlier (Reinders et al., 1998; Pedruzzi et al., 2000; Garrett and Broach, 1989). PCR-based gene deletions (*rim15Δ::kanMX* transformed into JK9-3da, KT1960, and W303-1A to create IP11, IP31, and CDV115, respectively; *ras2Δ::kanMX* transformed into SP1 to create IP16; *sit4Δ::TRP1* transformed into AR1-1B to create FD6; *cdc35Δ::kanMX* and *pde2Δ::TRP1* transformed into CDV147 [KT1960 X KT1961] to create CDV173; *sch9Δ::TRP1* transformed into W303-1A to create TVH301; and *sch9Δ::LEU2* transformed into CDV115 to create RJ201) and tagging of chromosomal *RIM15* (*RIM15-myc13-kanMX* transformed in KT1960 to create VW1) were done as described (Longtine et al., 1998). The homozygous *rim15Δ::kanMX/rim15Δ::kanMX* strain IP37 was created by PCR-based deletion of *RIM15* in CDV147, sporulation of the resulting heterozygous diploid, and mating of appropriate *rim15Δ::kanMX* haploids following tetrad analysis. The isogenic strains CDV80-2D and CDV80-15A are segregants of strain CDV80 that was created by mating S7-7A X S7-5A-derived NB13-1D and SGP406 (Reinders et al., 1998). Strain CDV173-3A (*MATa cdc35Δ::kanMX pde2Δ::TRP1* [pCDV548]) is a segregant of CDV173 that carried a low copy plasmid (*CEN, URA3; pCDV548*) expressing *cdc35-10* (amplified from strain PD6517). Mating of IP31 and CDV173-3A (both of isogenic background), followed by sporulation of the resulting diploid CDV177 yielded CDV177-3C (*MATa cdc35Δ::kanMX pde2Δ::TRP1 rim15Δ::kanMX* [pCDV548]). Growth on plates containing 5-FOA and 5 mM cAMP allowed selection of CDV177-3C that had lost pCDV548.

GFP- and GST-tagged versions of Rim15 were expressed under the control of the *ADH1* and *GAL1* promoters from a low (pFD633) and high (pCDV487) copy number plasmid, respectively. Plasmids YEp213-*RAS2^{Val19}*, pADH1-*Msn2-myc9*, and pSEY18-*TOR1-1* (pPW2) were described earlier (Broek et al., 1987; Görner et al., 1998; Hellwiell et al., 1994). Strains were grown at 30°C (except the *tap42-11* mutant, which was grown at 24°C) in standard rich medium (YPD) with 2% glucose or synthetic medium with 2% glucose (SD), 4% galactose (SGal), or 2% raffinose (SRaf) as carbon source (Burke et al., 2000). Rapamycin (dissolved in 90% ethanol/10% Tween-20) was added to the media at a final concentration of 2 $\mu\text{g ml}^{-1}$ for GFP-Rim15 localization studies and 0.2 $\mu\text{g ml}^{-1}$ for all other experiments.

Immunoblot Analyses

For immunoblot analyses, cells expressing GST-Rim15 from the *GAL1* promoter were grown to early logarithmic phase in SRaf medium. Expression of GST-Rim15 was induced by growth in SGal for 3 hr, followed by 3 hr in YPD. After that, cells were either treated for 20 min with rapamycin (+rap) or with the drug vehicle alone (–rap). Protein extracts were prepared using a standard postalkaline extraction method (Figure 3C, lanes 1 and 2 and 7–10), or a whole-cell extraction method as described (Figure 3C, lanes 3–6; Reinders et al., 1998). GST-Rim15 fusion proteins from whole-cell extracts were bound to glutathione agarose beads, washed extensively, eluted with 5 mM glutathione, and subjected to standard immunoblot analysis. Dephosphorylation of eluted GST-Rim15 was done by a 15 min incubation at 37°C with 1 unit of alkaline phosphatase (Roche Diagnostics). In control reactions, phosphatase inhibitors (10 mM NaF, 10 mM p-nitrophenylphosphate, 10 mM sodiumpyrophosphate, and 10 mM β -glycerophosphate) were added.

Miscellaneous

Northern analyses, trehalose measurements, flow cytometry, and indirect immunofluorescence were performed as described (Reinders et al., 1998; Burke et al., 2000). Glucose was measured using the GOD-PAP kit (HUMAN, GmbH).

Acknowledgments

We thank M. Hall, S. Harashima, and K. Tatchell for yeast strains and N. Bürckert and R. Bisig for technical assistance. This work was supported by grants of the Fund for Scientific Research-Flanders and the Research Fund of the Katholieke Universiteit Leuven to J.W. and the Swiss National Science Foundation to C.D.V. (631-62731.00).

Received: July 7, 2003

Revised: October 14, 2003

Accepted: October 22, 2003

Published: December 18, 2003

References

- Beck, T., and Hall, M.N. (1999). The TOR signalling pathway controls nuclear localization of nutrient-regulated transcription factors. *Nature* **402**, 689–692.
- Broek, D., Toda, T., Michaeli, T., Levin, L., Birchmeier, C., Zoller, M., Powers, S., and Wigler, M. (1987). The *S. cerevisiae CDC25* gene product regulates the RAS/adenylate cyclase pathway. *Cell* **48**, 789–799.
- Burke, D., Dawson, D., and Stearns, T. (2000). *Methods in Yeast Genetics*; 2000 Edition (Cold Spring Harbor New York: Cold Spring Harbor Laboratory Press).
- Cherkasova, V.A., and Hinnebusch, A.G. (2003). Translational control by TOR and TAP42 through dephosphorylation of eIF2 α kinase GCN2. *Genes Dev.* **17**, 859–872.
- Colomina, N., Liu, Y., Aldea, M., and Garí, E. (2003). TOR regulates the subcellular localization of Ime1, a transcriptional activator of meiotic development in budding yeast. *Mol. Cell. Biol.* **23**, 7415–7424.
- Crauwels, M., Donaton, M.C.V., Pernambuco, M.B., Winderickx, J., de Winde, J.H., and Thevelein, J.M. (1997). The Sch9 protein kinase in the yeast *Saccharomyces cerevisiae* controls cAPK activity and is required for nitrogen activation of the fermentable-growth-medium-induced (FGM) pathway. *Microbiol.* **143**, 2627–2637.
- Crespo, J.L., Powers, T., Fowler, B., and Hall, M.N. (2002). The TOR-controlled transcription activators GLN3, RTG1, and RTG3 are regulated in response to intracellular levels of glutamine. *Proc. Natl. Acad. Sci. USA* **99**, 6784–6789.
- Di Como, C.J., and Arndt, K.T. (1996). Nutrients, via the Tor proteins, stimulate the association of Tap42 with type 2A phosphatases. *Genes Dev.* **10**, 1904–1916.
- Düvel, K., Santhanam, A., Garrett, S., Schnepfer, L., and Broach, J.R. (2003). Multiple roles of Tap42 in mediating rapamycin-induced transcriptional changes in yeast. *Mol. Cell* **11**, 1467–1478.
- Fabrizio, P., Pozza, F., Pletcher, S.D., Gendron, C.M., and Longo, V.D. (2001). Regulation of longevity and stress resistance by Sch9 in yeast. *Science* **292**, 288–290.
- Garrett, S., and Broach, J. (1989). Loss of Ras activity in *Saccharomyces cerevisiae* is suppressed by disruptions of a new kinase gene, *YAK1*, whose product may act downstream of the cAMP-dependent protein kinase. *Genes Dev.* **3**, 1336–1348.
- Görner, W., Durchschlag, E., Martinez-Pastor, M.T., Estruch, F., Ammerer, G., Hamilton, B., Ruis, H., and Schüller, C. (1998). Nuclear localization of the C₂H₂ zinc finger protein Msn2p is regulated by stress and protein kinase A activity. *Genes Dev.* **12**, 586–597.
- Görner, W., Durchschlag, E., Wolf, J., Brown, E.L., Ammerer, G., Ruis, H., and Schüller, C. (2002). Acute glucose starvation activates the nuclear localization signal of a stress-specific yeast transcription factor. *EMBO J.* **21**, 135–144.
- Griffioen, G., Anghileri, P., Imre, E., Baroni, M.D., and Ruis, H. (2000). Nutritional control of nucleocytoplasmic localization of cAMP-dependent protein kinase catalytic and regulatory subunits in *Saccharomyces cerevisiae*. *J. Biol. Chem.* **275**, 1449–1456.
- Helliwell, S.B., Wagner, P., Kunz, J., Deuter-Reinhard, M., Henriquez, R., and Hall, M.N. (1994). TOR1 and TOR2 are structurally related and functionally similar but not identical phosphatidylinositol kinase homologues in yeast. *Mol. Biol. Cell* **5**, 105–118.
- Jacinto, E., and Hall, M.N. (2003). TOR signalling in bugs, brain and brawn. *Nat. Rev. Mol. Cell Biol.* **4**, 117–126.
- Jiang, Y., and Broach, J.R. (1999). Tor proteins and protein phosphatase 2A reciprocally regulate Tap42 in controlling cell growth in yeast. *EMBO J.* **18**, 2782–2792.
- Komeili, A., Wedaman, K.P., O'Shea, E.K., and Powers, T. (2000). Mechanism of metabolic control: target of rapamycin signaling links nitrogen quality to the activity of the Rtg1 and Rtg3 transcription factors. *J. Cell Biol.* **151**, 863–878.
- Liu, Z., Sekito, T., Spirek, M., Thornton, J., and Butow, R.A. (2003). Retrograde signaling is regulated by the dynamic interaction between Rtg2p and Mks1p. *Mol. Cell* **12**, 401–411.
- Longtine, M.S., McKenzie, A., 3rd, DeMarini, D.J., Shah, N.G., Wach, A., Brachat, A., Philippsen, P., and Pringle, J.R. (1998). Additional modules for versatile and economical PCR-based gene deletion and modification in *Saccharomyces cerevisiae*. *Yeast* **14**, 953–961.
- Lorenz, M.C., Pan, X., Harashima, T., Cardenas, M.E., Xue, Y., Hirsch, J.P., and Heitman, J. (2000). The G protein-coupled receptor Gpr1 is a nutrient sensor that regulates pseudohyphal differentiation in *Saccharomyces cerevisiae*. *Genetics* **154**, 609–622.
- Pedruzzi, I., Bürckert, N., Egger, P., and De Virgilio, C. (2000). *Saccharomyces cerevisiae* Ras/cAMP pathway controls post-diauxic shift element-dependent transcription through the zinc finger protein Gis1. *EMBO J.* **19**, 2569–2579.
- Reinders, A., Bürckert, N., Boller, T., Wiemken, A., and De Virgilio, C. (1998). *Saccharomyces cerevisiae* cAMP-dependent protein kinase controls entry into stationary phase through the Rim15p protein kinase. *Genes Dev.* **12**, 2943–2955.
- Sakumoto, N., Matsuoka, I., Mukai, Y., Ogawa, N., Kaneko, Y., and Harashima, S. (2002). A series of double disruptants for protein phosphatase genes in *Saccharomyces cerevisiae* and their phenotypic analysis. *Yeast* **19**, 587–599.
- Saxena, D., Kannan, K.B., and Brandriss, M.C. (2003). Rapamycin treatment results in GATA factor-independent hyperphosphorylation of the proline utilization pathway activator in *Saccharomyces cerevisiae*. *Eukaryot. Cell* **2**, 552–559.
- Schmidt, A., Beck, T., Koller, A., Kunz, J., and Hall, M.N. (1998). The TOR nutrient signalling pathway phosphorylates NPR1 and inhibits turnover of the tryptophan permease. *EMBO J.* **17**, 6924–6931.
- Stuart, J.S., Frederick, D.L., Varner, C.M., and Tatchell, K. (1994). The mutant type 1 protein phosphatase encoded by *gic7-1* from *Saccharomyces cerevisiae* fails to interact productively with the GAC1-encoded regulatory subunit. *Mol. Cell. Biol.* **14**, 896–905.
- Werner-Washburne, M., Braun, E., Johnston, G.C., and Singer, R.A. (1993). Stationary phase in the yeast *Saccharomyces cerevisiae*. *Microbiol. Rev.* **57**, 383–401.